Journal of Agricultural Faculty of Gaziosmanpasa University
Gaziosmanpaşa Üniversitesi Ziraat Fakültesi Dergisi
https://dergipark.org.tr/tr/pub/gopzfd

Research Article

JAFAG (2025) 42(2), 95-108
ISSN: 1300-2910
E-ISSN: 2147-8848
DOI: 10.55507/gopzfd.1652503

Drying of mango by intermittent and continuous infrared drying method

Ahmet Polat[1]*

[1]Bursa Uludag University, Faculty of Agriculture, Department of Biosystems Engineering, 16059, Bursa, Türkiye

***Corresponding author e-mail:** ahmetpolat@uludag.edu.tr

Received: 06.03.2025 Accepted: 20.04.2025

Abstract: This study examined the infrared drying process of mango slices at three power levels (300, 400, and 500 W) and three distinct intermittency ratios (PR=1, PR=1.5, and PR=2). The influence of these drying parameters on drying time, shrinkage, color stability, energy efficiency, rehydration capacity, and surface temperature was systematically assessed. Additionally, ten widely recognized mathematical thin-layer drying models were applied to the experimental data obtained under these conditions. The findings demonstrated that increasing infrared power while decreasing the intermittency ratio resulted in reduced drying times. Among the assessed models, the Midilli et al. model exhibited the highest accuracy in describing the infrared drying behavior of mango slices across different power levels and intermittency ratios. Furthermore, higher infrared power led to a decrease in L* values, indicating a darkening effect on the dried samples. Variations in infrared power did not significantly influence the shrinkage values of products dried at the same intermittency ratio ($p>0.5$). The surface temperature of mango products increased with decreasing the intermittency ratio and increasing the infrared power. Increasing the infrared power in PR=1 applications reduced energy consumption.

Keywords: Color, energy, intermittent infrared, mango

Kesikli ve sürekli kızılötesi kurutma yöntemiyle mangonun kurutulması

Öz: Bu çalışmada mango dilimlerinin kızılötesi kurutma işlemi üç güç seviyesinde (300, 400 ve 500 W) ve üç farklı aralıklılık oranında (PR = 1, PR = 1,5 ve PR = 2) incelenmiştir. Bu kurutma parametrelerinin kurutma süresi, büzülme, renk stabilitesi, enerji verimliliği, rehidrasyon kapasitesi ve yüzey sıcaklığı üzerindeki etkisi sistematik olarak değerlendirilmiştir. Ek olarak, bu koşullar altında elde edilen deneysel verilere on adet yaygın olarak kabul görmüş matematiksel ince tabaka kurutma modeli uygulanmıştır. Bulgular, kesiklilik oranını azaltırken kızılötesi gücün artırılmasının kurutma sürelerinin kısalmasıyla sonuçlandığını göstermiştir. Değerlendirilen modeller arasında Midilli ve ark. modeli, mango dilimlerinin kızılötesi kurutma davranışını farklı güç seviyeleri ve kesinti oranlarında tanımlamada en yüksek doğruluğu sergilemiştir. Ayrıca, daha yüksek kızılötesi güç L* değerlerinde düşüşe yol açarak kurutulan örneklerde koyulaşma etkisi olduğunu göstermiştir. Kızılötesi güçteki değişimler, aynı aralıklılık oranında kurutulan ürünlerin büzülme değerlerini önemli ölçüde etkilememiştir ($p>0,5$). Mango ürünlerinin yüzey sıcaklığı, aralık oranının azalması ve kızılötesi gücünün artmasıyla artmıştır. PR=1 uygulamalarında infrared gücünün artırılması enerji tüketimini azaltmıştır.

Anahtar kelimeler: Enerji, kesikli kızılötesi, mango, renk

1. Introduction

Fruits and vegetables are vital food sources, rich in key vitamins, antioxidant chemicals, and dietary fiber. Mango (*Mangifera indica* L.) is acknowledged as one of the most enjoyed tropical fruits globally. According to FAO (2025) production statistics, worldwide production of mangos, mangosteens, and guavas in 2023 was 61,107,091.76 tons, with the main production area being Asia with 71.8%. Mango is frequently consumed in both fresh and processed forms, valued for its distinct aroma and soft texture, making it a staple in various culinary applications.

Mango possesses health-enhancing attributes due to its polyphenols, vitamins, carotenoids, proteins, organic acids, and minerals. These bioactive components exhibit protective biological activities by showing antioxidative, anti-carcinogenic, anti-mutagenic, and

To cite this article: Polat, A. (2025). Drying of mango by intermittent and continuous infrared drying method. *Journal of Agricultural Faculty of Gaziosmanpasa University*, 42(2), 95-108. https://doi.org/10.55507/gopzfd.1652503

anti-atherosclerotic effects. Mango, due to its high moisture content, is susceptible to rapid deterioration and microbial proliferation when kept at ambient temperature. Additionally, it is unsuitable for cold storage at 4-5 °C, as temperatures below 10-12 °C can cause chilling injury, ultimately limiting its shelf life and contributing to post-harvest losses. In addition, hot water treatment is required as part of the quarantine requirement to accelerate the ripening process. These constraints increase post-harvest losses, reducing the commercial value of the fruit and generating large amounts of bio-waste that could potentially be converted into high-value products (Sogi et al., 2015; Sehrawat et al., 2018). Therefore, processing plays a crucial role in minimizing losses occurring after harvest in fruits. Among the oldest and most effective processing techniques, drying not only extends product availability beyond the typical harvest season but also provides several advantages such as minimizing losses after harvest, enhancing product value, prolonging shelf life, reducing volume, and facilitating transportation without requiring refrigeration. (Bhattacharjee et al., 2024). Dried products have gained increasing popularity as snacks due to their unique taste and aroma. They serve as a healthy alternative to fried snacks and are often preferred as substitutes for sweets and chocolates. Dried mango is primarily consumed as a snack and is commonly incorporated into breakfast cereals and energy bars. Additionally, it is used in various food products, including bakery items, desserts, and as a spice or additive (Izli et al., 2017).

Various methods are employed in the fruit processing industry to facilitate drying, including infrared, microwave, vacuum freeze, and hot air drying. Moreover, a combination of these techniques is frequently used to optimize the drying process and enhance product quality. Infrared drying, which has an important place in the processing of agricultural products, in principle provides homogeneous removal of water by generating heat energy directly in the internal structure through infrared radiation penetrating the material. Infrared drying offers several advantages, including even heat distribution, high energy efficiency, shorter drying durations, simple equipment structure, and improved final product quality (Li et al., 2023).

The drying process requires a significant amount of energy, contributing to ~20-25% of the total energy usage within the food industry. The increasing demand for premium-quality dried foods, along with the ongoing global energy crisis, has prompted researchers to explore and develop innovative drying technologies that can improve energy efficiency while maintaining product quality. In this context, intermittent drying has emerged as an important area of research that can be applied without increasing the initial investment required for drying systems (Kumar et al., 2014). Intermittent drying has been extensively applied to agricultural products and other heat-sensitive materials owing to its advantages in terms of energy efficiency, reduced processing time, and improved quality of the dried product. This approach mitigates thermo-hydric stress in grains, minimizes crack development, enhances overall quality, and reduces the drying length. Intermittency can be achieved by periodically modulating essential drying parameters, including the heat source, air mass flow rate, air velocity, air pressure, and temperature. These parameters may be alternately activated and deactivated, subjected to cyclic variations, or adjusted in response to external control signals (Barbosa de Lima et al., 2016).

A considerable body of research has explored various drying methods for mango preservation, including hot air drying, intermittent hot air drying, microwave-assisted drying, infrared drying, and freeze-drying (Izli et al., 2017; Abraham et al., 2020; Li et al., 2022). In these studies, different quality parameters such as color, antioxidant capacity, total phenolic content of mango were examined by drying with different methods. Despite these advancements, studies specifically focusing on intermittent infrared drying remain relatively scarce.

Infrared and intermittent infrared drying methods have been tested on different agricultural products. However, there are no studies on the drying of mango with these methods. In the present study, mango slices were subjected to drying under three different infrared power levels (300, 400, and 500 W) while employing varying intermittency ratios (PR=1, PR=1.5, and PR=2). The impact of these drying conditions on drying time, shrinkage, color stability, energy efficiency, rehydration capacity, and surface temperature was systematically analyzed. Furthermore, the drying characteristics of the mango slices were evaluated through ten distinct mathematical models to assess their suitability in predicting drying kinetics.

2. Materials and Methods

2.1. Sample preparation

Tommy Atkin mangoes (*Mangifera indica* L.) with a firm texture, green-purple skin, and light-yellow flesh were sourced from a local market. The mangoes, originally imported from Brazil, were selected based on their ripeness and their lack of microbial contamination or mechanical damage. Only uniform-sized and defect-free samples were chosen to ensure consistency in the drying process. Before drying, the mangoes were thoroughly washed with clean water to remove any surface residues and stored at 4±1°C under controlled conditions. This storage step was implemented to maintain freshness and prevent premature degradation. Prior to the drying procedure, samples were gradually brought to room temperature to avoid thermal shock. Following this preparation, the mangoes were peeled manually using a sanitized stainless-steel knife to ensure precision in cutting. They were then sliced into uniform cubes with dimensions of 10.604 × 10.675 × 3.929 mm using a calibrated food-grade cutter. For each drying experiment, precisely 35±0.01 g of mango samples was weighed and used. To determine the initial moisture content, randomly selected samples were subjected to drying in a laboratory oven

2.2. Dehydration process

The infrared drying process was conducted using a custom-designed drying system equipped with a 1500 W halogen infrared lamp, positioned in a longitudinal configuration (Figure 1). During the drying process, a consistent gap of 12 cm was maintained between the lamp and the mango samples. Both continuous and intermittent infrared drying methods were employed. Infrared power levels were adjusted to 300, 400, and 500 W, with intermittency ratios applied as follows: PR=1 (continuous drying), PR=1.5 (40 s on, 20 s off), and PR=2 (30 s on, 30 s off). The intermittency ratios were calculated based on the modifying equation proposed by Chua & Chou (2005):

$$Pulse\ Ratio = \frac{t_{on}+t_{off}}{t_{on}} \quad (1)$$

Where ton is the time when the infrared lamp is active and toff is the time when it is inactive.

The moisture content of fresh mango was then calculated as 4.84 g water/g dry matter (dry basis) to establish a reference for subsequent analyses. The drying procedure was carried out until the mango samples attained a final moisture content of 0.1 g water/g dry matter on a dry basis. To monitor the weight reduction over time, measurements were recorded at 10-minute intervals using a Shimadzu (Japan) digital balance with a precision of 0.01 g, immediately after the samples were removed from the drying chamber.

Figure 1. Designed infrared oven used in the experiments

2.3. Mathematical modeling

Numerous mathematical models have been developed to predict the drying behavior of food products. In this study, drying curves were analyzed using ten widely recognized thin-layer semi-theoretical and empirical models, as outlined in Table 1. These models are among the most frequently applied in literature. Within these models, 't' represents drying time, while 'k,' 'k_0,' and 'k_1' are defined as drying rate constants (1/min). Additionally, 'a,' 'b,' 'c,' 'g,' and 'n' serve as model coefficients. Eq. (2) was used to calculate the moisture content (MR) value used in the modeling studies (Xiao et al., 2014).

$$MR = \frac{M_t - M_e}{M_0 - M_e} \quad (2)$$

Where Mt, M0 and Me represent the moisture content at time t, time “0” and equilibrium, respectively. Since Me is relatively small compared to Mt or M0, Equation (2) is often simplified to Eq. (3) (Balbay & Şahin, 2012).

$$MR = \frac{M_t}{M_0} \quad (3)$$

2.4. Determination of shrinkage ratio

Shrinkage is typically quantified as the ratio of the sample's volume after drying to its initial volume before the drying process. Shrinkage values were calculated using Eq. (4) with a digital caliper before and after drying of five different mango cubes from different regions (Yan et al., 2008).

$$S = \frac{V_d}{V_0} \times 100 \quad (4)$$

Where Vd and V0 represent the post-dry and pre-dry volume, respectively.

Table 1. Thin layer mathematical modeling equations are to be used for the comparison of the moisture ratio values

No	Model name	Model	References
1	Henderson and Pabis	$MR = a\exp(-kt)$	Caliskan & Dirim (2015)
2	Newton	$MR = \exp(-kt)$	Pirnazari et al. (2016)
3	Page	$MR = \exp(-kt^n)$	Sacilik & Unal (2017)
4	Logarithmic	$MR = a\exp(-kt) + c$	Amiri Chayjan & Shadidi(2014)
5	Two term	$MR = a\exp(-k_0 t) + b\exp(-k_1 t)$	Bhattacharya et al. (2015)
6	Two term exponential	$MR = a\exp(-kt) + (1-a)\exp(-kat)$	Ergün et al. (2016)
7	Wang and Singh	$MR = 1 + at + bt^2$	Belghith et al. (2016)
8	Diffusion Approach	$MR = a\exp(-kt) + (1-a)\exp(-kbt)$	Perea-Flores et al. (2012)
9	Verma et al	$MR = a\exp(-kt) + (1-a)\exp(-gt)$	Taşkın et al. (2018)
10	Midilli et al.	$MR = a\exp(-kt^n) + bt$	Midilli et al. (2002)

2.5. Color measurement

The color characteristics of fresh and infrared-dried mango samples subjected to different treatment conditions were assessed using a Hunter Lab colorimeter to ensure precise and standardized measurements. The color attributes of fresh mango samples were denoted as L_0*, a_0*, and b_0*, while those of dried samples were expressed as L*, a*, and b*. To track the alterations in color during the drying process, several key parameters were calculated based on L*, a*, and b* values. These included total color difference (ΔE), chroma (C), hue angle (h°), whitening index (WI) and browning index (BI) which serve as essential indicators of color transformation in food products. Chroma, often referred to as the saturation index, represents the depth or purity of a color and is directly related to its intensity and vividness. Higher chroma values indicate more saturated and intense colors, whereas lower values suggest duller appearances. Another critical aspect of color evaluation in food science is the hue angle (h°), which defines the specific shade of a color perceived by the human eye. The hue angle is measured in radians and provides insight into color classification. A hue angle of 0 or 2π radians corresponds to red tones, while π/2 radians indicate yellow hues. Additionally, π radians are associated with green shades, whereas 3π/2 radians represent blue tones (Sharifian et al., 2013).

$$C = \sqrt{a^{*2} + b^{*2}} \quad (5)$$

$$h = tan^{-1}\left(\frac{b^*}{a^*}\right) \quad (6)$$

$$\Delta E = \sqrt{(L_0^* - L^*)^2 + (a_0^* - a^*)^2 + (b_0^* - b^*)^2} \quad (7)$$

$$WI = 100 - \sqrt{(100 - L^*)^2 + (a^*)^2 + (b^*)^2} \quad (8)$$

$$BI = \frac{[100(x-0.31)]}{0.172}, \text{where } x = \frac{(a^* + 1.75L^*)}{(5.645L^* + a^* - 3.012b^*)} \quad (9)$$

2.6. Energy analyses

The energy consumption (Ec) of the infrared drying system employed in the experiments was measured in kilowatt-hours (kWh) using a power meter (EU TS-836A; Floureon, China). To assess the overall efficiency of the drying process, several key performance indicators were calculated, including specific energy consumption (SEC), moisture extraction rate (MER), and specific moisture extraction rate (SMER), in accordance with Eqs. (10-12) (Baysal et al., 2015).

$$SEC = \frac{Total\ energy\ supplied\ in\ drying\ process\ (kWh)}{Amount\ of\ water\ removed\ during\ drying\ (kg)} \quad (10)$$

$$SMER = \frac{Amount\ of\ water\ removed\ during\ drying\ (kg)}{Total\ energy\ supplied\ in\ drying\ process\ (kWh)} \quad (11)$$

$$MER = \frac{Amount\ of\ water\ removed\ during\ drying\ (kg)}{Drying\ time\ (h)}. \quad (12)$$

The SEC parameter represents the total energy required to remove one kilogram of water from the sample, making it a critical factor in evaluating the energy efficiency of the drying system. The SMER metric, on the other hand, quantifies the amount of moisture removed per kilowatt-hour of energy consumed, providing insight into the system's performance in terms of energy utilization. Meanwhile, the MER value indicates the amount of moisture removed per unit of time (kg/hour), effectively reflecting the drying system's capacity and operational efficiency.

2.7. Rehydration measurement

Dried mango slices were rehydrated in glass beakers with distilled water for 14 hours at ambient

temperature (20 °C) (Askari et al., 2006). This rehydration process was performed in three replicates for each treatment to ensure accuracy and reproducibility. Once the 14-hour rehydration period was completed, the samples were carefully removed from the beakers and placed on absorbent filter paper to eliminate any remaining surface moisture. To determine their final weight, the rehydrated samples were weighed using a high-precision balance with a fine measurement scale. The rehydration capacity (RC) values were computed using the designated formula. In this equation, W1 represents the sample's initial dry weight, whereas W2 corresponds to its weight after rehydration.

$$Rehydration\ Capacity\ (\%) = \frac{W_2 - W_1}{W_1} \times 100 \qquad (13)$$

2.8. Determination of surface temperature

The surface temperature of the drying material was carefully measured at specific intervals using a high-precision infrared thermometer (62 Max+, Fluke) to ensure accuracy and consistency (Ghenai et al., 2023). To obtain reliable data, product temperature readings were taken from four predetermined points, with each measurement consistently recorded from the same locations, and the average values were used.

2.9. Statistical assessment

The experimental data collected from the drying process were documented and structured using MS Excel. For statistical evaluations, variance analysis and a single comparison test were conducted through JMP (Version 7, USA) at a 5% significance level. Additionally, the drying behavior of the samples was analyzed using MATLAB (MathWorks Inc., Natick, MA) to develop suitable mathematical models. To assess the agreement between experimental data and thin-layer drying models, several statistical indicators were employed. These included the coefficient of determination (R^2), chi-square (χ^2, Eq. 14), and root mean square error (RMSE, Eq. 15), following the methodology outlined by Bal et al. (2011).

$$\chi^2 = \frac{\sum_{i=1}^{N}(MR_{exp,i} - MR_{pre,i})^2}{N - z} \qquad (14)$$

$$RMSE = \sqrt{\frac{\sum_{i=1}^{N}(MR_{pre,i} - MR_{exp,i})^2}{N}} \qquad (15)$$

Here, MRexp,i and MRpre,i represent the experimentally measured and predicted moisture ratios, respectively, while i indicates the observation index. Furthermore, N corresponds to the total number of experimental data points, whereas z denotes the number of independent variables within the model.

3. Results and Discussion

3.1. Drying times

Figure 2 presents the changes in moisture content over time for mango samples dried under varying infrared power levels (300, 400, and 500 W) and different intermittency ratios (PR=1, PR=1.5, and PR=2).

The data illustrates how moisture content gradually decreases throughout the drying process, depending on the applied power and intermittency conditions. The results indicated that moisture content decreased progressively as drying time increased. Drying times for mango samples in drying applications where 300 W infrared power was used and the intermittency ratio was 1, 1.5, and 2 were found to be 100, 140, and 170 minutes, respectively. The results showed that an increase in the intermittency ratio led to a longer drying time for the products. In intermittent drying, the drying time was prolonged due to the longer toff time, i.e., less exposure to infrared rays. However, considering the active infrared working time (ton), shorter working time was obtained in the intermittent method compared to the continuous system since evaporation continued at the toff time (Rekik et al., 2021). Considering the total time (ton+toff), the continuous system took a shorter time. The same situation was valid for 400 and 500 W infrared drying. In their infrared drying study on potato and carrot at varying intermittency ratios, Chua & Chou (2005) found that higher intermittency ratios resulted in shorter drying times. These results are similar to the results of our study. In drying applications with an intermittent ratio of 1, mango products were dried in 100, 60, and 40 minutes at 300, 400, and 500 W infrared power, respectively. An increase in infrared power resulted in a reduction in drying time. As anticipated, the application of higher infrared power led to increased heat absorption by the product, which in turn elevated the product temperature, enhanced the mass transfer driving force, accelerated the drying rate, and ultimately resulted in a reduced overall drying time (Kayran & Doymaz, 2017).

In accordance with the results of this study, the phenomenon of decreasing drying time with increasing infrared power was observed in the studies of Doymaz (2017) on mango, Salehi, & Kashaninejad (2018) on grapefruit and Ghaboos et al. (2016) on pumpkin slices.

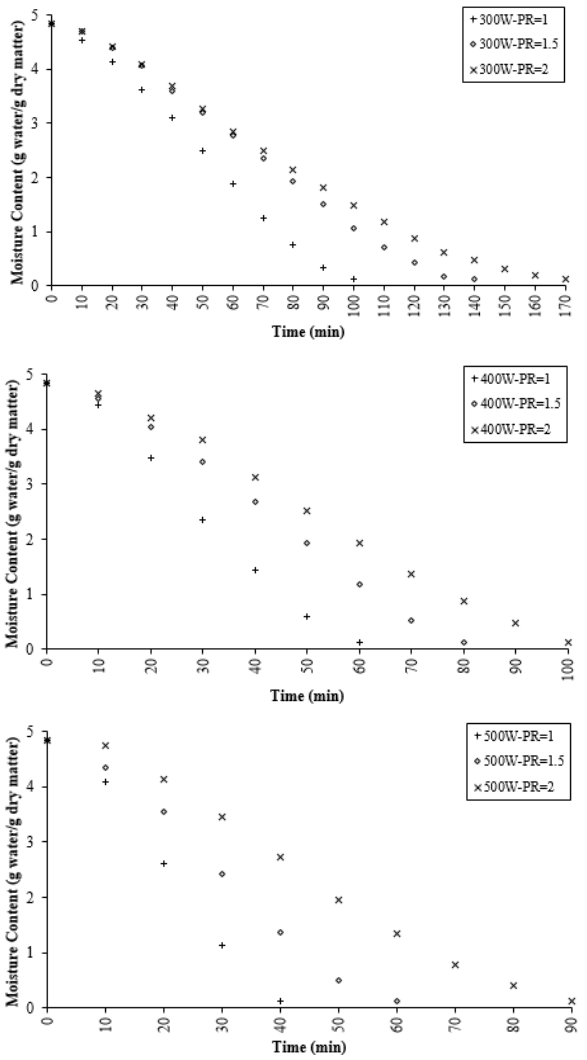

Figure 2. Variation of moisture content of mango samples dried by different infrared methods with time

3.2. Mathematical modeling evaluations

In this study, the thin-layer drying behavior of mango samples was investigated under three different intermittency ratios (PR = 1, 1.5, and 2) and varying infrared power levels (300, 400, and 500W). Experimental drying data were transformed into dimensionless moisture content (MR) and analyzed using the drying models listed in Table 1. The estimated model parameters and statistical evaluations for all drying conditions are presented in Tables 2, 3, and 4. To determine the most suitable model, nonlinear regression analysis was employed, considering the highest coefficient of determination (R^2), the lowest chi-squared (χ^2), and root mean square error (RMSE) values. The evaluated models demonstrated high R^2 values, ranging from 0.8606 to 0.999 indicating their strong capability in characterizing the drying kinetics of mango samples. Among these models, the Midilli et al. model consistently achieved the highest R^2 values, the lowest χ^2, and RMSE values across all drying conditions. Consequently, this model was identified as the most reliable representation of the infrared drying characteristics of mango samples at different power levels and intermittency ratios

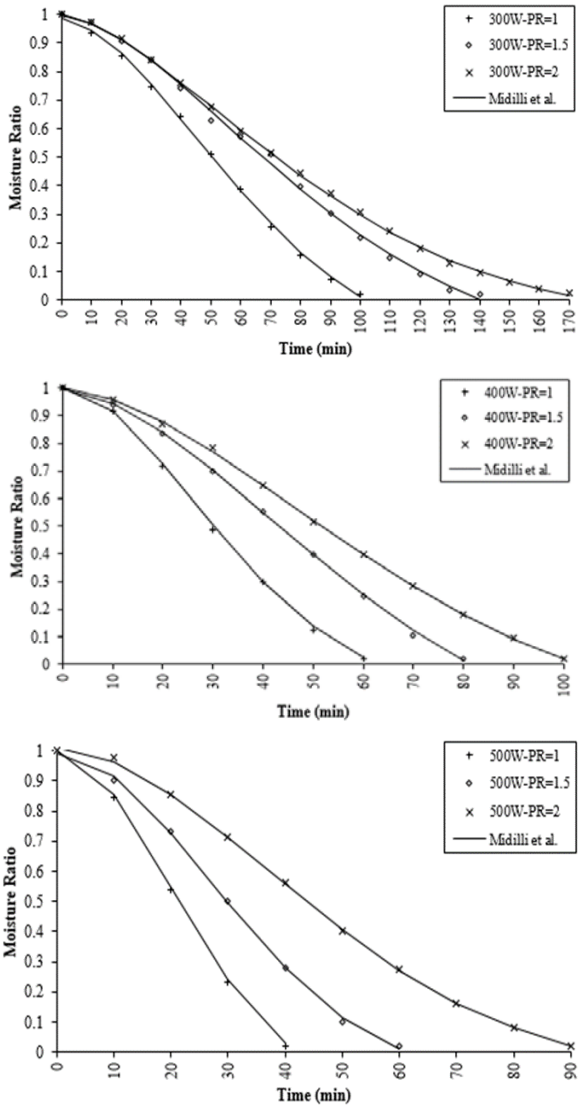

Figure 3. Comparison of the time variation of experimentally obtained moisture content values of mango samples dried by different infared methods with the model of Midilli et al.

Figure 3 presents the moisture content variations estimated by the Midilli et al. model in relation to drying time for mango samples dried using thin-layer infrared techniques. The results demonstrate that this model closely aligns with experimental data. Similarly, El-Mesery et al. (2024) investigated apple drying under different infrared conditions and identified the Midilli et al. model as the most effective in representing the drying curves of apple slices across all tested

parameters. Furthermore, Doymaz (2014) examined the drying kinetics of tomato slices at varying infrared power levels and found that the Midilli et al. model provided the most accurate fit. The findings of these studies corroborate the results obtained in this research.

3.3. Shrinkage

During the drying process, food materials frequently experience shrinkage, a physical phenomenon that significantly influences the final product's texture and taste, ultimately affecting consumer satisfaction (Mahiuddin et al., 2018). Table 5 presents the shrinkage values of mango samples dried under different infrared power levels and intermittency ratios. Shrinkage values varied between 22.160 % and 13.095 %. In 400 and 500 W infrared drying applications, the shrinkage value with the change of intermittency ratio did not have a statistical significance ($p>0.05$). Products dried at 300 W-PR=1 exhibited higher shrinkage values than those dried at 300 W-PR=1.5. However, when compared to the shrinkage values of samples dried at 300 W-PR=2, no statistically significant difference was detected ($p>0.05$). In addition, in 400 and 500 W drying applications, no statistical difference was observed in the shrinkage values with the change of PR values ($p>0.05$). This indicates that the applied intermittency ratio is generally not greatly affected by the product structural collapse phenomenon. Moreover, when the intermittency ratio remained constant, variations in infrared power levels did not lead to any statistically significant changes in shrinkage values ($p>0.05$). Shrinkage was closely associated with the moisture content, as the removal of water from the tissues led to pressure imbalances between the interior and exterior regions, resulting in mechanical stresses that induced structural collapse. However, the power levels (watt values) applied during the experiments did not exhibit a significant effect on these pressure-induced stresses (Supmoon & Noomhorm, 2013). In a similar study, Wang et al. (2014) found that squid samples dried under different infrared power conditions showed no significant differences in shrinkage percentage. Their findings agree with the results obtained in this study.

3.4. Evaluation of color results

The color values of fresh and infrared-dried mango slices, subjected to varying intermittency ratios and power levels, are summarized in Table 6. The initial color measurements for fresh samples were identified as L_0^* = 69.622 ± 0.478, a_0^* = 6.336 ± 0.029, and b_0^* = 68.252 ± 0.127. During the drying process, a decreasing trend was observed in L* and b* values, whereas a* values exhibited an upward trend. The observed increase in a* values, accompanied by decreases in L* and b* values, can be primarily attributed to the progression of enzymatic and particularly non-enzymatic browning reactions. In addition, the thermal degradation of pigments such as chlorophyll and carotenoids likely contributed to the overall color shift (Doymaz et al., 2016). Similarly, Yao et al. (2020) reported a decline in L* values and an increase in a* values in mango samples subjected to far-infrared drying, aligning with the results of this study. The 300 W-PR=2 treatment yielded the L* value closest to that of fresh mango, whereas the lowest L* value was found in the 500 W-PR=1 application. In 400 W and 500 W drying conditions, L* values showed a decreasing trend as the intermittency ratio increased, indicating a darkening effect. The rise in a* values indicate a greater intensity of red coloration in the dried mango samples. In samples dried at intermittency ratios of PR=1 and PR=1.5, a* values increased with the rise in infrared power, whereas the lowest a* values were found in mango samples dried at 300 W. These results align with the findings of Doymaz et al. (2016) in their study on jujube fruit drying. Regarding b* values, the lowest values at each infrared power level were recorded in samples dried under PR=1 conditions. The b* values most like those of fresh mango were observed in the 300 W-PR=2, 400 W-PR=1.5, and 400 W-PR=2 applications. Doymaz (2015) reported a similar reduction in b* values during the infrared drying of carrots, attributing this to a decrease in yellowness caused by infrared-induced thermal effects. The decline in b* values may be attributed to the breakdown of carotenoids, non-enzymatic Maillard reactions, and the development of brown-colored compounds. For the dried mango samples, chroma (C) and hue angle (h°) values were recorded within the ranges of 61.419 ± 0.171 to 49.297 ± 0.853 and 83.226 ± 0.039 to 73.456 ± 0.484, respectively. The greatest deviation in C value from that of fresh mango was observed in the 500 W-PR=1 application. A significant variation in hue angle values was observed across all drying conditions ($p<0.05$), with the 300 W-PR=2 treatment yielding the closest hue angle to that of fresh mango. The browning index (BI) was employed to evaluate the extent of non-enzymatic browning reactions such as Maillard reactions, ascorbic acid oxidation, and/or enzymatic

browning processes (Aradwad et al., 2023). In contrast, the whiteness index (WI) was used as an indicator of product discoloration, where higher WI values generally reflect lower degrees of browning. The WI values of mango samples were significantly influenced ($p<0.05$) by the applied infrared power levels. However, no significant correlation was observed between WI and BI under different intermittency ratios at constant power levels. Among the treatments, samples dried at 400 W (PR = 1, 1.5, and 2) exhibited lower WI values and correspondingly higher BI values compared to other drying conditions. This inverse relationship suggests a negative correlation between WI and BI. As expected, fresh samples demonstrated higher WI values, while BI values tended to increase as a result of the drying process. These findings are in agreement with the results reported by Cerezal-Mezquita & Bugueño-Muñoz (2022) in their carrot drying experiments. Total color difference (ΔE), a widely used colorimetric parameter for assessing color changes in food processing, was lowest in the 300 W-PR=2 treatment, indicating the highest similarity to fresh mango. At a constant infrared power level, ΔE values decreased as the intermittency ratio increased, and at a fixed intermittency ratio, ΔE values declined with lower infrared power. Color retention was found to be closely associated with the internal temperature of the mango samples. Under continuous infrared exposure, elevated surface temperatures can accelerate pigment denaturation, thereby leading to more pronounced color degradation (Rekik et al., 2021).

In line with these results, Mongpraneet et al. (2002) and Ghaboos et al. (2016) observed that increased infrared power led to a more significant total color change in their studies on pumpkin and Welsh onion drying.

3.5. Evaluation of energy analysis

Table 7 displays the energy consumption values for mango samples dried under various infrared power levels and intermittency ratios. Among the drying processes, the 500 W-PR=2 treatment exhibited the highest energy consumption, whereas the 400 W-PR=2 application recorded the lowest.

Here, energy consumption showed differences according to the infrared active operating time.

Table 2. Results of statistical analyzes on modeling moisture content and drying time of mango samples dried at 300W infrared power

No	300 W PR:1				300 W PR:1.5				300 W PR:2			
	Model Coefficient	R^2	RMSE	$\chi^2(10^{-4})$	Model Coefficient	R^2	RMSE	$\chi^2(10^{-4})$	Model Coefficient	R^2	RMSE	$\chi^2(10^{-4})$
1	a=1.1287 k=0.0189	0.9164	0.108	114.9543	a=1.149 k=0.0143	0.9258	0.0985	97.6926	a=1.141 k=0.0132	0.9503	0.0784	62.1567
2	k=0.0166	0.891	0.117	134.7126	k=0.0123	0.8951	0.1129	128.2717	k=0.0115	0.9247	0.0936	88.9506
3	k=0.000308 n=1.982	0.9942	0.0286	7.8880	k=0.000214 n=1.928	0.9955	0.0242	5.7195	k=0.000454 n=1.720	0.9983	0.0143	2.0883
4	a=14.461 k=0.0007645 c=-13.4153	0.9929	0.0333	11.1639	a=6.404 k=0.0013 c=-5.3506	0.9931	0.0313	13.6204	a=2.008 k=0.0046 c=-0.9467	0.993	0.0304	9.5236
5	a=-11.356 k_o=0.0431 b=12.328 k_1=0.0388	0.9801	0.0597	34.7741	a=14.944 k_o=0.0291 b=-13.975 k_1=0.0317	0.9847	0.0486	25.8741	a=10.587 k_o=0.0252 b=-9.611 k_1=0.0283	0.9936	0.0301	9.1340
6	a=0.0004 k=41.5993	0.8908	0.1234	149.9014	a=2.168 k=0.0217	0.9799	0.0513	27.6937	a=2.112 k=0.0194	0.9907	0.0339	11.5853
7	a=-0.0091 b=-0.0000124	0.9911	0.0352	12.4679	a=-0.0071 b=0.00000293	0.9894	0.0372	14.9551	a=-0.0076 b=0.00000907	0.9892	0.0366	13.8000
8	a=-22.316 k=0.9482 b=0.042	0.891	0.1308	168.4037	a=4.5459 k=0.000541 b=-2.4208	0.9893	0.0389	16.2382	a=19.204 k=0.0255 b=1.0619	0.9933	0.0298	8.9281
9	a=-0.293 k=3.0325 g=0.0218	0.9458	0.0922	83.9789	a=19.732 k=0.029 g=0.0309	0.984	0.0475	24.3897	a=0.030 k=0.0115 g=0.0115	0.9247	0.0997	100.811
10	a=0.9889 k=0.000467 n=1.804 b=-0.0014	0.9992	0.0123	1.6005	a=0.9971 k=0.000384 n=1.736 b=-0.000906	0.9993	0.0106	3.2697	a=0.9985 k=0.000675 n=1.604 b=-0.000376	0.9997	0.0062	0.4450

Table 3. Results of statistical analyzes on modeling moisture content and drying time of mango samples dried at 400W infrared power

No	400 W PR:1				400 W PR:1.5				400 W PR:2			
	Model Coefficient	R^2	RMSE	$\chi^2(10^{-4})$	Model Coefficient	R^2	RMSE	$\chi^2(10^{-4})$	Model Coefficient	R^2	RMSE	$\chi^2(10^{-4})$
1	a=1.1139 k=0.0313	0.912	0.1251	150.7330	a=1.128 k=0.0219	0.9027	0.1206	145.4157	a=1.139 k=0.0183	0.9159	0.1079	115.7365
2	k=0.0281	0.891	0.1271	155.5015	k=0.0192	0.8754	0.1276	162.7655	k=0.0158	0.8858	0.1192	141.2854
3	k=0.000663 n=2.054	0.9978	0.0196	3.3555	k=0.000258 n=2.111	0.9944	0.0288	8.2671	k=0.000251 n=2.017	0.9967	0.0213	4.4556
4	a=15.120 k=0.0012 c=-14.0729	0.9884	0.0508	25.7351	a=24.354 k=0.000551 c--23.2909	0.9913	0.039	15.6307	a=107.158 k=0.0000979 c=-106.1141	0.9925	0.0341	11.8434
5	a=15.842 k_o=0.0686 b=-14.850 k_1=0.0749	0.9879	0.06	33.9564	a=14.653 k_o=0.0471 b=-13.6749 k_1=0.0517	0.9778	0.0682	46.8926	a=1.311 k_o=0.0213 b=-0.311 k_1=10.9989	0.9497	0.0946	89.0149
6	a=2.259 k=0.0512	0.9839	0.0536	27.2432	a=0.0003356 k=57.167	0.8753	0.1365	186.2357	a=2.197 k=0.0287	0.9793	0.0536	28.3028
7	a=-0.0155 b=-0.0000266	0.9853	0.0512	25.2453	a=-0.0093 b=-0.0000433	0.9923	0.034	12.1852	a=-0.0084 b=-0.0000187	0.99	0.0372	14.2225
8	a=-19.0497 k=0.0739 b=0.934	0.9878	0.0521	25.5883	a=-26.0518 k=0.0000382 b=12.8483	0.9812	0.0573	33.0019	a=4.5809 k=0.0061 b=0.6817	0.9437	0.0936	87.0552
9	a=33.626 k=0.0702 g=0.0731	0.9878	0.0521	25.6259	a=20.685 k=0.0474 g=0.0505	0.9773	0.0629	39.8078	a=20.387 k=0.0386 g=0.0411	0.9838	0.0503	24.9336
10	a=1.0031 k=0.001 n=1.886 b=-0.0013	0.9997	0.0099	1.9903	a=0.9974 k=0.000426 n=1.885 b=-0.0022	0.9998	0.0066	0.7649	a=0.999 k=0.000417 n=1.828 b=-0.0013	0.9998	0.0053	0.4249

Table 4. Results of statistical analyzes on modeling moisture content and drying time of mango samples dried at 500W infrared power

No	500 W PR:1				500 W PR:1.5				500 W PR:2			
	Model Coefficient	R^2	RMSE	$\chi^2(10^{-4})$	Model Coefficient	R^2	RMSE	$\chi^2(10^{-4})$	Model Coefficient	R^2	RMSE	$\chi^2(10^{-4})$
1	a=1.0859 k=0.0437	0.8624	0.1522	222.6649	a=1.111 k=0.0317	0.8882	0.1296	166.6295	a=1.147 k=0.0218	0.909	0.1116	125.5142
2	k=0.0403	0.8832	0.1402	188.9209	k=0.0285	0.8872	0.1302	168.3466	k=0.0189	0.8878	0.1239	154.8842
3	k=0.000877 n=2.197	0.996	0.0258	6.819	k=0.000536 n=2.119	0.9968	0.0219	4.4024	k=3.24E-04 n=2.034	0.9984	0.0149	1.6815
4	a=164.454 k=0.000153 c=-163.4292	0.9748	0.0652	38.3688	a=22.336 k=0.000818 c=-21.2938	0.9797	0.0553	31.3343	a=5.825 k=0.0023 c=-4.7581	0.9838	0.0471	23.3693
5	a=-16.715 k_o=0.112 b=-17.718 k_1=0.1029	0.9386	0.1187	98.7480	a=1.461 k_o=0.0414 b=-0.4605 k_1=2.4011	0.9195	0.11	119.4394	a=38.113 k_o=0.0477 b=-37.195 k_1=0.0496	0.9789	0.0538	30.3372
6	a=2.355 k=0.0762	0.9743	0.0657	41.1141	a=2.248 k=0.0514	0.9736	0.063	38.7177	a=2.250 k=0.0346	0.9844	0.0462	21.0343
7	a=-0.02 b=-0.000129	0.9849	0.0504	23.6618	a=-0.0157 b=-0.0000253	0.9805	0.0542	30.0072	a=-0.0107 b=-0.00000949	0.9789	0.0537	30.2383
8	a=6.2282 k=0.0133 b=0.728	0.8947	0.1331	166.9741	a=23.4177 k=0.0121 b=0.954	0.9	0.1226	149.3810	a=2.4781 k=0.0164 b=0.9035	0.8606	0.1381	192.4443
9	a=224.402 k=0.1047 g=0.1054	0.9692	0.072	55.9823	a=29.267 k=0.0706 g=0.074	0.9741	0.0623	38.0277	a=7.202 k=0.000322 g=-0.0014	0.9757	0.0576	35.0847
10	a=0.9999 k=0.0013 n=1.991 b=-0.0026	0.9999	0.000052	3.7661	a=0.9914 k=0.000680 n=2.009 b=-0.0011	0.9987	0.0142	2.0676	a=1.0096 k=0.000532 n=1.881 b=-0.000672	0.9993	0.0096	0.6770

Table 5. Rehydration capacity and shrinkage values of mango samples dried at different intermittency ratios

Product	Rehydration capacity (%)	Shrinkage (%)
300 W-PR=1	2.581 (0.139)^{bc}	19.749 (5.031)^{a}
300 W-PR=1.5	2.469 (0.060)^{c}	13.095 (2.507)^{b}
300 W-PR=2	2.350 (0.099)^{cd}	18.959 (2.424)^{ab}
400 W-PR=1	2.967 (0.134)^{a}	22.160 (5.715)^{a}
400 W-PR=1.5	2.777 (0.077)^{ab}	18.662 (4.425)^{ab}
400 W-PR=2	2.360 (0.229)^{cd}	20.624 (5.824)^{a}
500 W-PR=1	2.824 (0.216)^{a}	20.357 (5.966)^{a}
500 W-PR=1.5	2.795 (0.090)^{ab}	17.445 (4.641)^{ab}
500 W-PR=2	2.218 (0.039)^{d}	19.274 (4.810)^{a}

Unlike our study, Puente-Díaz et al. (2013) found that energy consumption decreased with infrared power in their study. The different infrared powers used here may determine the efficiency in drying time. For specific energy consumption (SEC), the highest value (10.681 kWh/kg) was found in the 500 W-PR=2 application, whereas the lowest SEC value (9.215 kWh/kg) was noted in the 400 W-PR=2 condition. A decreasing trend in SEC values was observed as infrared power increased in PR=1 drying applications, a finding that aligns with the results of Bualuang et al. (2013) in their study on parboiled rice drying. Table 7 indicates that SMER values varied between 0.094 kg/kWh and 0.109 kg/kWh, with the values observed in 500 W-PR=1, 500 W-PR=2, and 300 W-PR=2 applications being relatively similar. SMER is a key metric in assessing the energy performance of drying operations, as higher moisture removal rates indicate greater efficiency in energy utilization. (Boateng & Yang, 2021). Moreover, the moisture extraction rate (MER) is directly influenced by drying duration. In 300 W PR=1, PR=1.5 and PR=2 applications, MER values were found as 0.017, 0.012 and 0.010 kg/h, respectively. Analysis of MER values revealed that, at a constant infrared power level, MER decreased with an increase in the intermittency ratio. In 300 W-PR=1.5 application, the MER value was 0.012 kg/h, in 400 W-PR=1.5 application it was 0.021 kg/h and in 500 W-PR=1.5 applications it was 0.029 kg/h. From these results, at a constant intermittency ratio, MER values declined as infrared power was reduced. These findings are consistent with the drying times recorded in the study Similar to the results of our study, Altay et al. (2019) determined that MER values decreased with increasing drying time for all drying methods and conditions.

3.6. Rehydration

Rehydration plays a fundamental role in evaluating the overall quality of dried products, as it reflects the physical and chemical transformations that take place during the drying process (Aral & Beşe, 2016).

Table 6. Color values of fresh and dried mango samples with different intermittent ratios

Drying conditions	Color parameters							
	*L**	*a**	*b**	*C*	*α°*	*ΔE*	*BI*	*WI*
Fresh	69.622 (0.478)^{a}	6.336 (0.029)^{h}	68.252 (0.127)^{a}	68.252 (0.127)^{a}	84.739 (0.031)^{a}	-	204.373 (3.286)^{a}	25.024 (0.268)^{g}
300 W-PR=1	65.714 (0.205)^{c}	7.330 (0.032)^{g}	57.548 (0.121)^{d}	58.012 (0.123)^{d}	82.783 (0.027)^{c}	11.440 (0.076)^{d}	166.794 (1.487)^{f}	32.612 (0.196)^{d}
300 W-PR=1.5	65.64 (0.239)^{c}	8.094 (0.055)^{f}	59.296 (0.235)^{c}	59.846 (0.240)^{c}	82.269 (0.030)^{d}	9.959 (0.264)^{b}	177.169 (1.341)^{d}	30.991 (0.189)^{c}
300 W-PR=2	67.858 (1.326)^{b}	7.248 (0.011)^{g}	60.636 (0.389)^{b}	61.068 (0.386)^{b}	83.226 (0.039)^{b}	7.947 (0.633)^{a}	172.627 (4.492)^{e}	30.980 (0.348)^{c}
400 W-PR=1	58.376 (0.527)^{g}	10.274 (0.405)^{bc}	55.608 (0.083)^{e}	56.550 (0.074)^{e}	79.573 (0.412)^{h}	17.381 (0.322)^{f}	199.173 (3.899)^{b}	29.781 (0.365)^{d}
400 W-PR=1.5	61.838 (0.129)^{e}	9.378 (0.022)^{d}	60.526 (0.447)^{b}	61.248 (0.440)^{b}	81.233 (0.078)^{e}	11.387 (0.252)^{d}	207.929 (3.603)^{a}	27.836 (0.420)^{f}
400 W-PR=2	63.294 (0.212)^{d}	10.374 (0.034)^{b}	60.536 (0.172)^{b}	61.419 (0.171)^{b}	80.316 (0.036)^{g}	10.766 (0.200)^{c}	199.785 (1.256)^{b}	28.449 (0.139)^{e}
500 W-PR=1	56.860 (0.768)^{h}	14.062 (0.064)^{a}	47.248 (0.500)^{g}	49.297 (0.853)^{g}	73.456 (0.484)^{j}	25.767 (1.085)^{h}	162.406 (3.781)^{g}	34.485 (0.503)^{a}
500 W-PR=1.5	60.082 (0.711)^{f}	10.160 (0.044)^{c}	51.350 (0.147)^{f}	52.346 (0.148)^{f}	78.848 (0.042)^{i}	19.790 (0.303)^{g}	164.221 (3.912)^{fg}	34.170 (0.503)^{a}
500 W-PR=2	62.144 (0.082)^{e}	9.158 (0.064)^{e}	57.080 (0.500)^{d}	57.810 (0.501)^{d}	80.926 (0.058)^{f}	13.740 (0.379)^{e}	184.360 (3.195)^{c}	30.898 (0.437)^{c}

a-j Means superscript with different alphabets in the same column differ significantly ($p \leq 0.05$).

Table 7. Energy values of mango slices dried with different treatments

Product	*EC (kWh)*	*SEC (kWh/kg)*	*SMER (kg/kWh)*	*MER (kg/h)*
300 W-PR=1	0.297	10.366	0.096	0.017
300 W-PR=1.5	0.281	9.808	0.102	0.012
300 W-PR=2	0.284	9.913	0.101	0.010
400 W-PR=1	0.285	9.948	0.101	0.029
400 W-PR=1.5	0.290	10.122	0.099	0.021
400 W-PR=2	0.264	9.215	0.109	0.017
500 W-PR=1	0.283	9.878	0.101	0.043
500 W-PR=1.5	0.270	9.424	0.106	0.029
500 W-PR=2	0.306	10.681	0.094	0.019

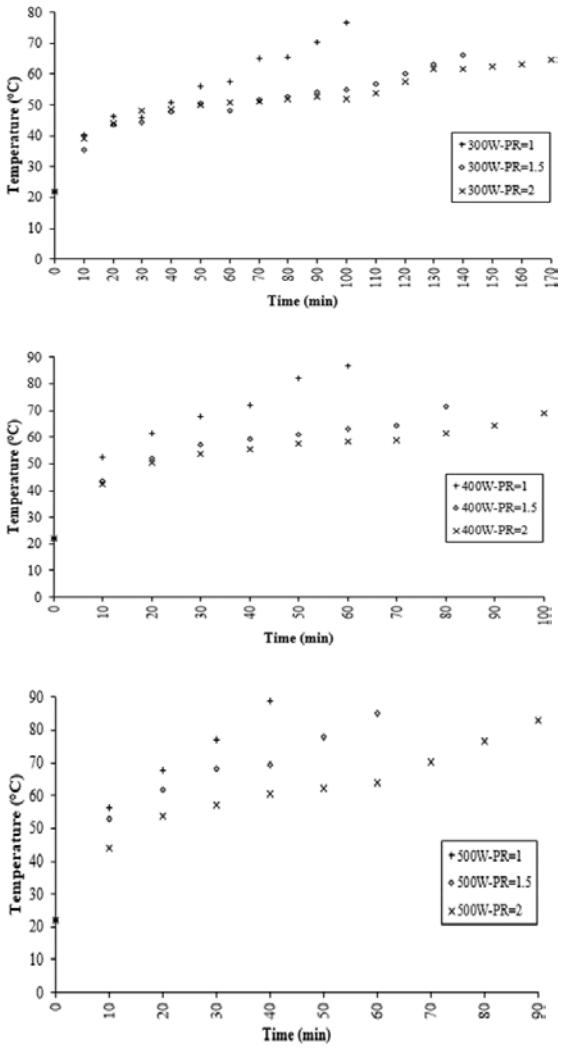

Figure 4. Surface temperature values of mango slices dried by different processes

The rehydration capacity measurements obtained from the dried mango samples are summarized in Table 5. In the 300 W drying applications, variations in the intermittency ratio did not significantly influence rehydration capacity. Likewise, at 400 W and 500 W infrared power levels, the rehydration capacity of samples dried under PR=1 and PR=1.5 conditions exhibited no statistically significant variation ($p>0.05$). However, samples dried at PR=2 exhibited lower rehydration capacity compared to those dried at lower intermittency ratios. Additionally, increasing the infrared power from 400 W to 500 W across all intermittency ratios did not lead to a significant change in rehydration capacity. While no notable variation was detected in rehydration capacity for PR=2 applications with increasing infrared power, a decrease in rehydration capacity was observed in samples dried at 300 W in PR=1 and PR=1.5 applications when infrared power was increased to 400 W and 500 W. These findings are consistent with earlier studies. Aydogdu et al. (2015) found that increasing infrared power enhanced rehydration capacity in their research on the drying of eggplant. Similarly, Nathakaranakule et al. (2010) obtained comparable results in their research on longan drying.

3.7. Surface temperature

The surface temperatures of mango samples dried under different infrared power and intermittency conditions are presented in Figure 4. The data indicate that surface temperatures initially increased logarithmically, then showed a brief decline at a certain point before rising linearly toward the final stage of the drying process. Mango samples dried under the 500 W-PR=1 condition exhibited the highest surface temperature (88.97 °C). For samples dried at 500 W-PR=1.5 and 500 W-PR=2, surface temperatures were measured as 84.87 °C and 83.1 °C, respectively. As the intermittency ratio increased, the samples were exposed to infrared radiation intermittently rather than continuously, resulting in lower surface temperatures compared to continuous drying conditions. Adjusting the intermittency ratio and infrared exposure time helped mitigate excessive heating of the biomaterial. During the "relaxation" periods (when the infrared radiation was off), surface temperatures decreased, as noted by Chua & Chou (2005). The surface temperature of mango samples dried at 300 W-PR=2 was 64.57 °C, which increased to 68.93 °C at 400 W and further to 83.1 °C at 500 W. This demonstrates that increasing

infrared power at a constant intermittency ratio led to higher surface temperatures. Similar trends have been reported by Zhu & Pan (2009) and Datta & Ni (2002), who found that surface temperatures increased with higher infrared intensity.

4. Conclusion

The drying time was analyzed to assess the drying behavior of mango slices, focusing on shrinkage ratio, color, energy analysis, rehydration, surface temperature, and the effects of varying infrared powers and intermittency ratios. The longest drying duration (170 minutes) was recorded under the 300 W-PR=2 condition, whereas the shortest duration was noted in the 500 W-PR=1 application. Among the examined models, the Midilli et al. model demonstrated the highest accuracy in describing the thin-layer drying characteristics of mango samples. Products obtained from PR=2 treatments at different infrared power levels had the lowest L* values. For products dried at 300 W, rehydration capacity remained largely unaffected by variations in the intermittency ratio, whereas the lowest rehydration capacity values for 400 W and 500 W drying conditions were obtained at PR=2. Moreover, increasing the infrared power from 300 W to 400 W led to an improvement in rehydration capacity. For samples dried at the same intermittency ratio, variations in infrared power did not lead to a statistically significant difference in shrinkage values. At the highest infrared power and the lowest intermittency ratio, mango products reached the highest surface temperature value. The highest SMER value was found in the 400 W-PR=2 treatments due to the low energy required to dry the products. According to the results, while intermittent infrared drying caused a minor extension in the total drying time, the reduced thermal exposure of the product had positive effects. However, research on this drying method remains incomplete. Further experimental and theoretical investigations are required to enhance product quality and energy efficiency in intermittent infrared drying.

Conflict of interest

The author declares no conflicts of interest.

Authorship contribution statement

A.P.: Concept, design, data collection or processing, statistical analyses, literature search, writing, review and editing.

References

Abraham, T. F., Marcel, E., & Alexis, K. (2020). Intermittent drying of mango slices (*Mangifera indica* L.)" Amelie": A new model. *American Journal of Food Science and Technology, 8(3),* 81-86. https://doi.org/10.12691/ajfst-8-3-1

Altay, K., Hayaloglu, A. A., & Dirim, S. N. (2019). Determination of the drying kinetics and energy efficiency of purple basil (*Ocimum basilicum* L.) leaves using different drying methods. *Heat and Mass Transfer, 55,* 2173-2184. https://doi.org/10.1007/s00231-019-02570-9.

Amiri Chayjan, R., & Shadidi, B. (2014). Modeling high-moisture Faba bean drying in fixed and semi-fluidized bed conditions. *Journal of Food Processing and Preservation, 38(1)*, 200-211. https://doi.org/10.1111/j.1745-4549.2012.00766.x.

Aral, S., & Beşe, A. V. (2016). Convective drying of hawthorn fruit (*Crataegus spp*.): Effect of experimental parameters on drying kinetics, color, shrinkage, and rehydration capacity. *Food chemistry, 210*, 577-584. https://doi.org/10.1016/j.foodchem.2016.04.128.

Aradwad, P. P., Thirumani Venkatesh, A. K., & Mani, I. (2023). Infrared drying of apple (Malus domestica) slices: Effect on drying and color kinetics, texture, rehydration, and microstructure. *Journal of Food Process Engineering, 46(2),* e14218. https://doi.org/10.1111/jfpe.14218.

Askari, G. R., Emam-Djomeh, Z., & Mousavi, S. M. (2006). Effects of combined coating and microwave assisted hot-air drying on the texture, microstructure and rehydration characteristics of apple slices. *Food Science and Technology International, 12(1)*, 39-46. https://doi.org/10.1177/1082013206062480.

Aydogdu, A., Sumnu, G., & Sahin, S. (2015). Effects of microwave-infrared combination drying on quality of eggplants. *Food and Bioprocess Technology, 8*, 1198-1210. https://doi.org/10.1007/s11947-015-1484-1.

Bal, L. M., Kar, A., Satya, S., & Naik, S. N. (2011). Kinetics of colour change of bamboo shoot slices during microwave drying. *International Journal of Food Science & Technology, 46(4)*, 827-833. https://doi.org/10.1111/j.1365-2621.2011.02553.x.

Balbay, A., & Şahin, Ö. (2012). Microwave drying kinetics of a thin-layer liquorice root. *Drying Technology, 30(8)*, 859-864. https://doi.org/10.1080/07373937.2012.670682.

Barbosa de Lima, A.G., Delgado, J.M.P.Q., Neto, S.R.F., Franco, C.M.R. (2016). *Intermittent Drying: Fundamentals, Modeling and Applications*. In: Delgado, J., Barbosa de Lima, A. (eds) Drying and Energy Technologies. Advanced Structured Materials, vol 63. Springer, Cham. https://doi.org/10.1007/978-3-319-19767-8_2.

Baysal, T., Ozbalta, N., Gokbulut, S., Capar, B., Tastan, O., & Gurlek, G. (2015). Investigation of effects of various drying methods on the quality characteristics of apple slices and energy efficiency. *Isı Bilimi ve Tekniği Dergisi, 35(1)*, 135-144.

Belghith, A., Azzouz, S., & ElCafsi, A. (2016). Desorption isotherms and mathematical modeling of thin layer drying kinetics of tomato. *Heat and Mass Transfer*, *52*, 407-419. https://doi.org/10.1007/s00231-015-1560-0.

Bhattacharjee, S., Mohanty, P., Sahu, J. K., & Sahu, J. N. (2024). A critical review on drying of food materials: recent progress and key challenges. *International Communications in Heat and Mass Transfer, 158*, 107863. https://doi.org/10.1016/j.icheatmasstransfer.2024.107863.

Bhattacharya, M., Srivastav, P. P., & Mishra, H. N. (2015). Thin-layer modeling of convective and microwave-convective drying of oyster mushroom (*Pleurotus ostreatus*). *Journal of Food Science and Technology*, *52*, 2013-2022. https://doi.org/10.1007/s13197-013-1209-2.

Boateng, I. D., & Yang, X. M. (2021). Osmotic, osmovacuum, sonication, and osmosonication pretreatment on the infrared drying of Ginkgo seed slices: Mass transfer, mathematical modeling, drying, and rehydration kinetics and energy consumption. *Journal of Food Science*, *86(10)*, 4577-4593. https://doi.org/10.1111/1750-3841.15916.

Bualuang, O., Tirawanichakul, Y., & Tirawanichakul, S. (2013). Comparative study between hot air and infrared drying of parboiled rice: Kinetics and qualities aspects. *Journal of Food Processing and Preservation, 37(6)*, 1119-1132. https://doi.org/10.1111/j.1745-4549.2012.00813.x.

Caliskan, G., & Dirim, S. N. (2017). Drying characteristics of pumpkin (Cucurbita moschata) slices in convective and freeze dryer. *Heat and Mass Transfer, 53*, 2129-2141. https://doi.org/10.1007/s00231-017-1967-x.

Cerezal-Mezquita, P., & Bugueño-Muñoz, W. (2022). Drying of carrot strips in indirect solar dehydrator with photovoltaic cell and thermal energy storage. *Sustainability, 14(4),* 2147. https://doi.org/10.3390/su14042147.

Chua, K. J., & Chou, S. K. (2005). A comparative study between intermittent microwave and infrared drying of bioproducts. *International Journal of Food Science & Technology, 40(1)*, 23-39. https://doi.org/10.1111/j.1365-2621.2004.00903.x.

Datta, A. K., & Ni, H. (2002). Infrared and hot-air-assisted microwave heating of foods for control of surface moisture. *Journal of Food Engineering*, *51(4)*, 355-364. https://doi.org/10.1016/S0260-8774(01)00079-6.

Doymaz, İ. (2014). Mathematical modeling of drying of tomato slices using infrared radiation. *Journal of Food Processing and Preservation*, 38(1), 389-396. https://doi.org/10.1111/j.1745-4549.2012.00786.x.

Doymaz, İ. (2015). Infrared drying kinetics and quality characteristics of carrot slices. *Journal of Food Processing and Preservation, 39(6)*, 2738-2745. https://doi.org/10.1111/jfpp.12524.

Doymaz, İ. (2017). Microwave and infrared drying characteristics of mango slices. *Celal Bayar University Journal of Science, 13(3)*, 681-688. https://doi.org/10.18466/cbayarfbe.339337.

Doymaz, İ., Karasu, S., & Baslar, M. (2016). Effects of infrared heating on drying kinetics, antioxidant activity, phenolic content, and color of jujube fruit. *Journal of Food Measurement and Characterization*, *10,* 283-291. https://doi.org/10.1007/s11694-016-9305-4.

El-Mesery, H. S., Ashiagbor, K., Hu, Z., & Rostom, M. (2024). Mathematical modeling of thin-layer drying kinetics and moisture diffusivity study of apple slices using infrared conveyor-belt dryer. *Journal of Food Science, 89(3)*, 1658-1671. https://doi.org/10.1111/1750-3841.16967.

Ergün, K., Çalışkan, G., & Dirim, S. N. (2016). Determination of the drying and rehydration kinetics of freeze dried kiwi (*Actinidia deliciosa*) slices. *Heat and Mass Transfer*, *52(12)*, 2697-2705. https://doi.org/10.1007/s00231-016-1773-x.

FAO. (2025). The food and agriculture organization corporate statistical database. Retrieved from https://www.fao.org/faostat/en/#data/QCL/visualize. (Accessed 14 April 2025).

Ghaboos, S. H. H., Ardabili, S. M. S., Kashaninejad, M., Asadi, G., & Aalami, M. (2016). Combined infrared-vacuum drying of pumpkin slices. *Journal of Food Science and Technology, 53*, 2380-2388. https://doi.org/10.1007/s13197-016-2212-1.

Ghenai, C., Rejeb, O., Sinclair, T., Almarzouqi, N., Alhanaee, N., & Rossi, F. (2023). Evaluation and thermal performance of cool pavement under desert weather conditions: Surface albedo enhancement and carbon emissions offset. *Case Studies in Construction Materials*, *18*, e01940. https://doi.org/10.1016/j.cscm.2023.e01940.

Izli, N., İzli, G., & Taskin, O. (2017). Influence of different drying techniques on drying parameters of mango. *Food Science and Technology, 37(4)*, 604-612. https://doi.org/10.1590/1678-457X.28316.

Kayran, S., & Doymaz, İ. (2017). Infrared drying and effective moisture diffusivity of apricot halves: Influence of pretreatment and infrared power. *Journal of Food Processing and Preservation, 41(2)*, e12827. https://doi.org/10.1111/jfpp.12827.

Kumar, C., Karim, M. A., & Joardder, M. U. (2014). Intermittent drying of food products: A critical review. *Journal of Food Engineering, 121*, 48-57. https://doi.org/10.1016/j.jfoodeng.2013.08.014.

Li, D., Dai, T., Chen, M., Liang, R., Liu, W., Liu, C., ... & Deng, L. (2023). Role of maturity status on the quality and volatile properties of mango fruits dried by infrared radiation. *Food Bioscience, 52*, 102497. https://doi.org/10.1016/j.fbio.2023.102497.

Li, D., Deng, L., Dai, T., Chen, M., Liang, R., Liu, W., ... & Sun, J. (2022). Ripening induced degradation of pectin and cellulose affects the far infrared drying kinetics of mangoes. *Carbohydrate Polymers, 291*, 119582. https://doi.org/10.1016/j.carbpol.2022.119582.

Mahiuddin, M., Khan, M. I. H., Kumar, C., Rahman, M. M., & Karim, M. A. (2018). Shrinkage of food materials during drying: Current status and challenges. *Comprehensive Reviews in Food Science and Food Safety, 17(5)*, 1113-1126.

https://doi.org/10.1111/1541-4337.12375.

Midilli, A., Kucuk, H., & Yapar, Z. (2002) A new model for single-layer drying. *Drying Technology, 20(7)*, 1503-1513. https://doi.org/10.1081/DRT-120005864.

Mongpraneet, S., Abe, T., & Tsurusaki, T. (2002). Accelerated drying of welsh onion by far infrared radiation under vacuum conditions. *Journal of Food Engineering*, *55(2)*, 147-156. https://doi.org/10.1016/S0260-8774(02)00058-4.

Nathakaranakule, A., Jaiboon, P., & Soponronnarit, S. (2010). Far-infrared radiation assisted drying of longan fruit. *Journal of Food Engineering*, *100(4)*, 662-668. https://doi.org/10.1016/j.jfoodeng.2010.05.016.

Palamutoğlu, R. (2020). Antibrowning effect of commercial and acid-heat coagulated whey on potatoes during refrigerated storage. *Journal of Food Science, 85(11),* 3858-3865. https://doi.org/10.1111/1750-3841.15468.

Perea-Flores, M. J., Garibay-Febles, V., Chanona-Pérez, J. J., Calderón-Domínguez, G., Méndez-Méndez, J. V., Palacios-González, E., & Gutiérrez-López, G. F. (2012). Mathematical modelling of castor oil seeds (Ricinus communis) drying kinetics in fluidized bed at high temperatures. *Industrial Crops and Products, 38*, 64-71. https://doi.org/10.1016/j.indcrop.2012.01.008.

Puente-Díaz, L., Ah-Hen, K., Vega-Gálvez, A., Lemus-Mondaca, R., & Scala, K. D. (2013). Combined infrared-convective drying of murta (Ugni molinae Turcz) berries: Kinetic modeling and quality assessment. *Drying Technology, 31(3),* 329-338. https://doi.org/10.1080/07373937.2012.736113.

Rekik, C., Besombes, C., Hajji, W., Gliguem, H., Bellagha, S., Mujumdar, A. S., & Allaf, K. (2021). Study of interval infrared Airflow Drying: A case study of butternut (*Cucurbita moschata*). *Lwt, 147,* 111486. https://doi.org/10.1016/j.lwt.2021.111486.

Sacilik, K., & Unal, G. (2005). Dehydration characteristics of Kastamonu garlic slices. *Biosystems Engineering, 92(2),* 207-215. https://doi.org/10.1016/j.biosystemseng.2005.06.006.

Salehi, F., & Kashaninejad, M. (2018). Mass transfer and color changes kinetics of infrared-vacuum drying of grapefruit slices. *International Journal of Fruit Science, 18(4)*, 394-409. https://doi.org/10.1080/15538362.2018.1458266.

Sehrawat, R., Nema, P. K., & Kaur, B. P. (2018). Quality evaluation and drying characteristics of mango cubes dried using low-pressure superheated steam, vacuum and hot air drying methods. *Lwt, 92*, 548-555. https://doi.org/10.1016/j.lwt.2018.03.012.

Sharifian, F., Modarres-Motlagh, A., Komarizade, M. H., & Nikbakht, A. M. (2013). Colour change analysis of fig fruit during microwave drying. *International Journal of Food Engineering, 9(1)*, 107-114. https://doi.org/10.1515/ijfe-2012-0211.

Sogi, D. S., Siddiq, M., & Dolan, K. D. (2015). Total phenolics, carotenoids and antioxidant properties of Tommy Atkin mango cubes as affected by drying techniques. *LWT-Food Science and Technology, 62(1)*, 564-568. https://doi.org/10.1016/j.lwt.2014.04.015.

Supmoon, N., & Noomhorm, A. (2013). Influence of combined hot air impingement and infrared drying on drying kinetics and physical properties of potato chips. *Drying Technology, 31(1),* 24-31. https://doi.org/10.1080/07373937.2012.711792.

Taşkın, O., İzli, G., & İzli, N. (2018) Convective drying kinetics and quality parameters of european cranberrybush. *Journal of Agricultural Science*, *24(3)*, 349-358. https://doi.org/10.15832/ankutbd.456654.

Wang, Y., Zhang, M., Mujumdar, A. S., & Chen, H. (2014). Drying and quality characteristics of shredded squid in an infrared-assisted convective dryer. *Drying Technology*, *32(15)*, 1828-1839. https://doi.org/10.1080/07373937.2014.952379.

Xiao, H. W., Law, C. L., Sun, D. W., & Gao, Z. J. (2014). Color change kinetics of American ginseng (*Panax quinquefolium*) slices during air impingement drying. *Drying Technology*, *32(4)*, 418-427. https://doi.org/10.1080/07373937.2013.834928.

Yan, Z., Sousa-Gallagher, M. J., & Oliveira, F. A. (2008). Shrinkage and porosity of banana, pineapple and mango slices during air-drying. *Journal of Food Engineering, 84(3)*, 430-440. https://doi.org/10.1016/j.jfoodeng.2007.06.004.

Yao, L., Fan, L., & Duan, Z. (2020). Effect of different pretreatments followed by hot-air and far-infrared drying on the bioactive compounds, physicochemical property and microstructure of mango slices. *Food Chemistry*, *305*, 125477. https://doi.org/10.1016/j.foodchem.2019.125477.

Zhu, Y., & Pan, Z. (2009). Processing and quality characteristics of apple slices under simultaneous infrared dry-blanching and dehydration with continuous heating. Journal of Food Engineering, 90(4), 441-452. https://doi.org/10.1016/j.jfoodeng.2008.07.015.